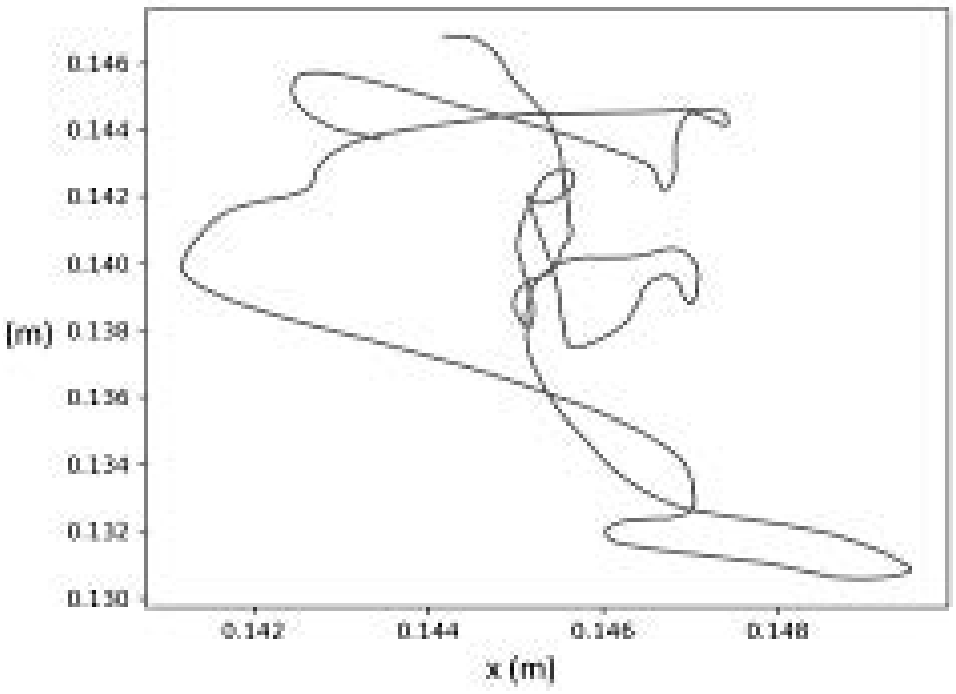

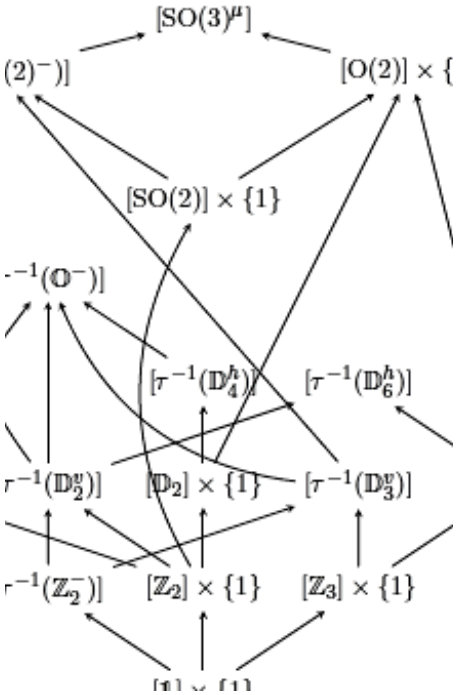

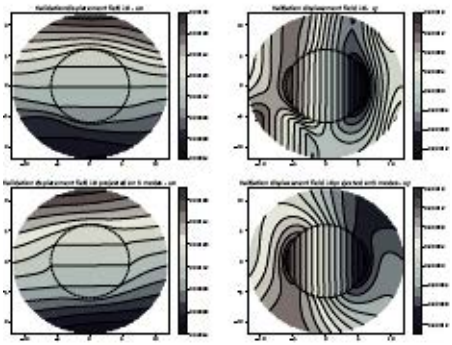

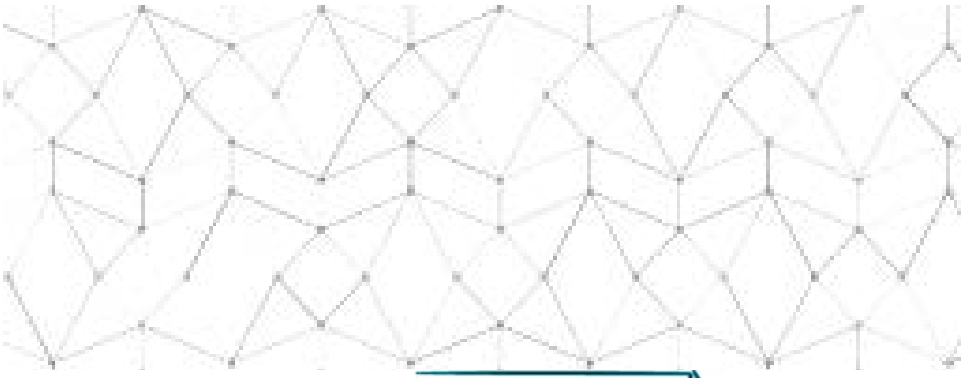

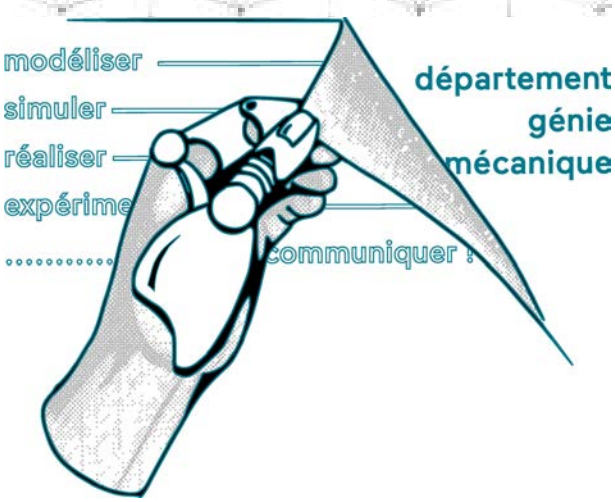

RESEARCH PROJECTS

STUDENTS OF THE DEPARTMENT OF MECHANICAL ENGINEERING

2019
20

ABSTRACT

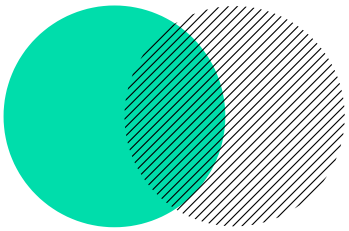

AUTOMATIC DETERMINATION OF MECHANICAL PATTERNS FOR PARSIMONIOUS MODELING OF MICROSTRUCTURES

KARIM AÏT AMMAR - LOUEN POTTIER
EMMANUEL BARANGER

TTER M1 2019-2020
FINAL DEFENCE OF RESEARCH PROJECTS
March 31, 2020, Cachan, France

école normale supérieure paris—saclay

Automatic determination of mechanical patterns for parsimonious modeling of microstructures

Karim AÏT AMMAR[*], Louen POTTIER[†], Emmanuel BARANGER[◇]

[*] [†] Département de génie mécanique
École Normale Supérieure Paris-Saclay
61 Avenue du Président Wilson, 94230 Cachan

[*] e-mail: karim.ait_ammar@ens-paris-saclay.fr

[†] e-mail: louen.pottier@ens-paris-saclay.fr

[◇] Université Paris-Saclay, ENS Paris-Saclay
CNRS, LMT - Laboratoire de Mécanique et Technologie
94235, Cachan, France
e-mail: emmanuel.baranger@ens-paris-saclay.fr

KEYWORDS: Principal Component Analysis, microstructures, finite elements, convolutional neural networks, machine learning

ABSTRACT

General context

The finite element method is widely used to compute displacement fields of microstructures because of its robustness. The key feature of this method is to use a vast set of simple elementary displacement fields to compute complex global displacement fields. Yet, one of the major drawbacks of this method is the lack of physical sense of the elementary fields it uses. In this study, we use two different and independent machine learning methods (Principal Component Analysis [1] and convolutional autoencoder neural networks [2]) to describe global displacement fields on microstructures using a limited set of rich displacement fields named modes.

Methods

Machine learning methods such as Principal Component Analysis (PCA) and convolutional neural networks were used to compute the displacement modes mentioned above. Algorithms based on such techniques need to be trained on large sets of data so as to be truly effective. Hence, a first step consisted in generating a significant training basis. To this end, about 3000 composite microstructures were randomly generated using a *Python* routine. The displacement responses of those microstructures to three pre-defined mechanical loads - traction, shearing and transversal shearing - were then computed using *Abaqus*, a finite element solver. Finally, the displacement fields near the fibers were projected on a unique extraction mesh (in order to make the results comparable) and saved in a database. Considering that each microstructure contained 7 fibers on average, the obtained database consisted of more than 70000 displacement fields. A few additional fields called validation fields were generated following the same principle for error computation. Once the data were acquired, the two methods were applied on the training base. For the PCA, The validation displacement fields were then projected on the most significant modes hence obtained, as shown on figure 2. The error induced by the projection was computed using the L^2 norm. At the same time,

convolutional neural networks were built with the described architecture described on Figure 1 using the *Python* library *pytorch-geometric* which contains several methods for deep learning on graphs data. The network aims to encode a given displacement field into a small dimension representation and then to decode it minimizing the reconstruction error. This architecture has been compared to a simpler fully-connected one.

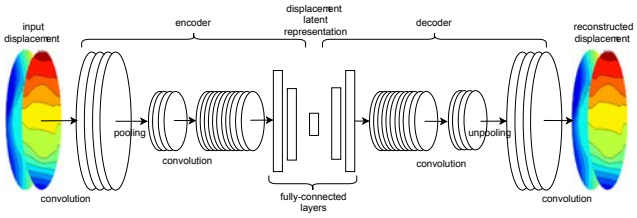

Figure 1: Choosen architecture for the convolutional autoencoder.

Results

Concerning the PCA method, the study reveals that complex displacement fields can be described by a few significant modes with a relatively low error (about 7.5% for three modes and 5.95% for five). Besides, it shows that smaller training bases yield similar results as larger bases, meaning that a satisfying set of displacement modes can be obtained with limited data. Furthermore, the obtained modes do bear physical sense, as one may clearly recognise a traction and a shearing field on Figure 2. Concerning the neural network method, results prove that convolutional networks are not only faster to train than fully-connected ones, but they also generate smoother displacement fields as shown on Figure 3.

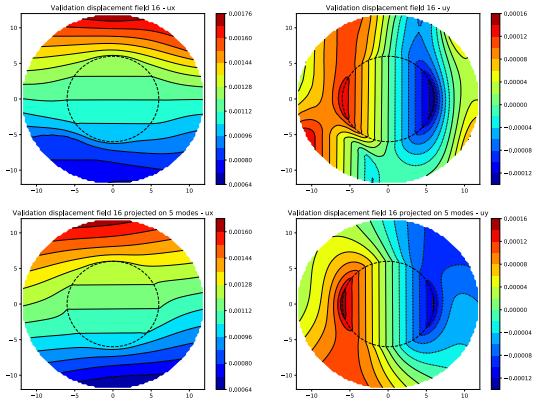

Figure 2: Projection of a validation displacement fields on the first 6 modes

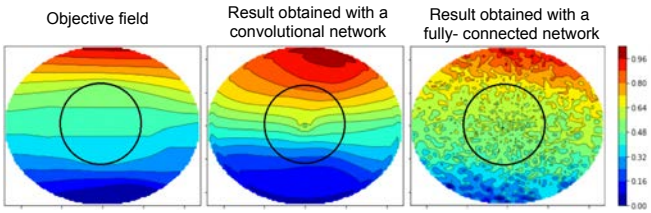

Figure 3: Norm of a validation field and its reconstructions obtained with the convolutional and the fully-connected networks trained with the same amount of data (1500 fields). Both latent representations have 10 dimensions.

REFERENCES

[1] J-A. Lee, M. Verleysen. *Nonlinear Dimensionality Reduction*. Springer (2007) - *DOI:10.1007/978-0-387-39351-3*

[2] K. Lee, K-T. Carlberg. *Model reduction of dynamical systems on nonlinear manifolds using deep convolutional autoencoders*. Journal of Computational Physics (2020) - *DOI:10.1016/j.jcp.2019.108973*

ELDERLY PERSON MEDICAL SUPERVISION USING AN INSTRUMENTED DOOR

PAUL LABAT - PIERRE-LOUIS CORDONNIER
BRUNO DENIS - GREGORY FARAUT

TER M1 2019-2020
FINAL DEFENCE OF RESEARCH PROJECTS
March 31, 2020, Cachan, France

école normale supérieure paris—saclay

TER M1 2019-2020
FINAL DEFENCE OF RESEARCH PROJECTS
March 31, 2020, Cachan, France

Elderly person medical supervision using an instrumented door.

Paul LABAT*, Pierre-Louis CORDONNIER†, Bruno DENIS◊ , Gregory Faraut◊

* DGM
ENS Paris Saclay
e-mail: paul.labat@ens-paris-saclay.fr

† DGM
ENS Paris Saclay
e-mail: pierre-louis.cordonnier@ens-paris-saclay.fr

◊ LURPA
ENS Paris Saclay
e-mail: bruno.denis@ens-paris-saclay.fr
e-mail: gregory.faraut@ens-paris-saclay.fr

KEYWORDS: old age; tonus; muscle power; measurement system, mobility-disability

ABSTRACT

General Information

Statistics show that the population is aging, and research assesses that elderly people are in better health when living at home compared to living in a nursing home [1]. The decision as to when a person should be put in such institution is decided case by case and under the advice of a doctor, often after the person suffered a fall and could not get up.

The aim of our study is to create a mechanical system that will be added to the door of an elderly person. This will be used by doctors to determine when a person is too disabled to live alone and is risking a fall that could cause injuries.

Such a system will measure a mechanical quantity that varies with the user's age. Exercise physiology research shows [2] that muscle power declines sooner and more rapidly than muscle strength, due to muscle loss with advancing age. Thus, we chose to instrument a door so that it could collect data on the power transmitted by the user when opening or closing it.

Part 1: Mechanical model

The first step was to make a mechanical model of the door and its opening. This model and the list of its variables shows that a system that can measure the position of the door in function of the time, is sufficient to determine the power transmitted by the door's user.

Part 2: conception and realization of the prototype

The second step was to choose the kinematic of the system. We studied two different kinematics that can support either longitudinal or rotational sensors, and a third that allows only the latter. These kinematics have to be compact, compatible with the sensors, and isostatic. We then ran an optimization algorithm for each one of the five configurations, using a criterion over the sensitivity of the measured data (length or angle). Thus, we had the best set of geometrical parameters for each kinematic, and the sensitivity of the associated measure, which we used to choose our kinematic (Figure

1). Knowing the kinematic and the dimensions of our system, we could design each part with Catia V5 and 3D print them. To design the different parts, we studied the influence of errors on each geometrical parameter so as to make sure that the most critical dimensions could be adjusted.

Part 3: data measurement and analysis

The third step was to create a database of door opening measurements in order to track the decline of the user's tonus. The system should be able to differentiate different users. Thus, we planned on using neuronal networks to analyze the data and recognize the users. Due to delays on the optimization phase, we have not been able to go through the manipulations yet and do not have any data to analyze. We had planned on doing it during the upcoming weeks, but considering the current situation, we are unsure whether we will be able to conclude on this part of the project.

Conclusion and further work

In the end, we were able to design and build a prototype of the system (Figure 2), but we have not had enough time to collect and analyze much data. This work should be completed with the data analysis part, but already guarantees that the data can be taken with a maximum precision.

This research is of critical importance considering the fact that it could improve the well-being of elderly persons. Further studies could implement a reeducation system that would control the amount of effort the user needs to produce to open the door.

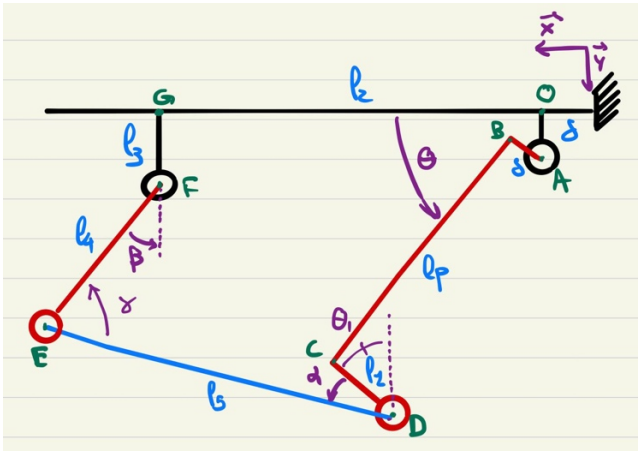

Figure 1: Kinematic plan.

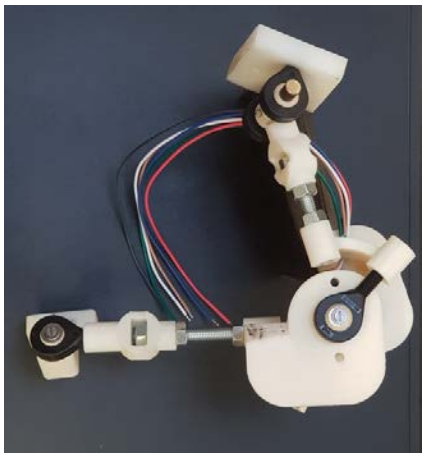

Figure 2: Photo of the prototype.

REFERENCES

[1] L. Calvet, N. Pradines. *État de santé et dépendance des personnes âgées en institution ou a domicile*. Études et Résultats, numéro 0988, décembre 2016.

[2] Kieran F. Reid, Roger A. Fielding. Skeletal Muscle Power: A Critical Determinant of Physical Functioning In Older Adults. *Exerc Sport Sci Rev* **Vol**: 40(1):4-12, 2012 January.

INNOVATIVE SCALE FOR LONGITUDINAL BALANCE MONITORING

MAXIME KACKZMAREK -
AMAURY BELLIER-GANIERE
BRUNO DENIS - GREGORY FARAUT

TER M1 2019-2020
FINAL DEFENCE OF RESEARCH PROJECTS
March 31, 2020, Cachan, France

école normale supérieure paris—saclay

Innovative scale for longitudinal balance monitoring

Maxime Kackzmarek[*], Amaury Bellier-Ganière[†]
Bruno Denis[◇], Grégory Faraut[□]

Département de Génie Mécanique
Ecole Normale Supérieure Paris-Saclay
61 Avenue du Président Wilson, 94230 Cachan

Lurpa
Ecole Normale Supérieure Paris-Saclay
61 Avenue du Président Wilson, 94230 Cachan

[*] maxime.kaczmarek@ens-paris-saclay.fr
[†] amaury.bellier-ganiere@ens-paris-saclay.fr
[◇] bruno.denis@ens-paris-saclay.fr
[□]gregory.faraut@ens-paris-saclay.fr

KEYWORDS: Stabilometry, machine learning, longitudinal balance monitoring.

ABSTRACT

General Information

The current ageing of the population is leading to an increasing demand for care among the elderly. While placing the elderly in retirement homes is a common solution to this issue, several studies show that keeping them in their homes as long as possible is beneficial for their health and more specifically for their autonomy [1]. In this context, in order to both preserve their health and to reduce the costs due to their growing need for health care, research has been carried out on home monitoring systems with a view to postpone elderly placement as much as possible. Among all the health indicators, stability has been reported as particularly reliable. Former research has focused on stability from a general point of view, but has failed to clearly link stabilometric indicators to specific disorders [2]. The aim of this study is to build a personal stabilometric platform measuring the position of the projection of the centre of gravity and reaction forces and torques.

Methodology

The activities involved in this project were the implementation of the stabilometric platform prototype and the calibration of the load cell sensors. Thus far, we were not able to perform the data analysis part of the study, as many unexpected technical problems were encountered during the manufacture of the scale. Concerning the implementation of the prototype, the first step was to create and manufacture the printed circuit board by choosing the adequate electrical components, in particular the load cells (Micro Load Cell CLZ635 (0-50 kg)), the instrumentation amplifiers (Burr-Brown, INA-125-P) and the analog-to-digital converter (Measurement computing, USB-1608FS-Plus). The calibration of the load cells consisted in determining the relation between the load and the tension issued by the sensor/amplifier/converter system. Each one of the sensor/amplifier/converter sets were found to be linear and were calibrated to have a $(0,100 \pm 0,002)\ V/kg$ gradient. The balance pan in itself is a square plate of steel, measuring 400 mm $\times$ 400 mm, with a thickness of 6 mm. This thickness was calculated to limit the bending of the plate to less than a millimetre under a 100 kg load. The four load cells were put under the pan, at the four corners, in order to maximise the precision of the measure of the centre of gravity. We developed a python script to gather the data and we saved them using the json format, which can be used in most of database programs. As a whole, the stabilometric platform cost about 100€.

Results

The relative measurement uncertainty of the output voltage of the analog-to-digital converter can be calculated as follows:

$$\varepsilon(V_{converter}) = \varepsilon(G_{converter}) + \varepsilon(G_{amplifier}) + \varepsilon(G_{sensor}) + \varepsilon(V_{power}) = 5,09\ \%$$

with $V_{converter}$ the tension output delivered by the analog-to-digital converter, $G_{converter}$ the gain of the analog-to-digital converter, $G_{amplifier}$ the gain of the instrumentation amplifier, G_{sensor} the gain of the sensor and V_{power} the tension of the power supply of the stabilometric platform.

The relative measurement uncertainty of the position of the projection of the centre of gravity on the platform can be deduced of it as follows:

$$\varepsilon(X_g) = \varepsilon\left(\sum_{i=1}^{4} m_i X_i\right) + \varepsilon(m_{tot}) = 10,4\%$$

with X_g the position of the projection of the centre of gravity on the scale plan, m_i the mass measured by the i-load cell, X_i the position of the i-load cell and m_{tot} the total mass measured by the stabilometric platform.

The main source of uncertainty is the power supply of the load cells (5V USB port) which is responsible for 79 % of the relative measurement uncertainty of the output voltage of the analog-to-digital converter. The results suggest that it is possible to obtain usable data for balance monitoring with a relatively cheap stabilometric platform, and therefore affordable for the general public.

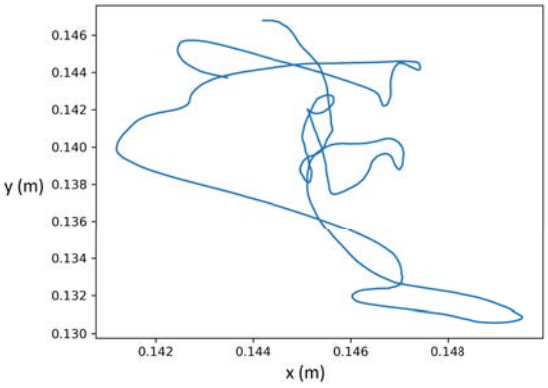

Figure 1: Evolution of the position of the projection of the centre of gravity on the scale for a 20 years old man standing still with his eyes opened

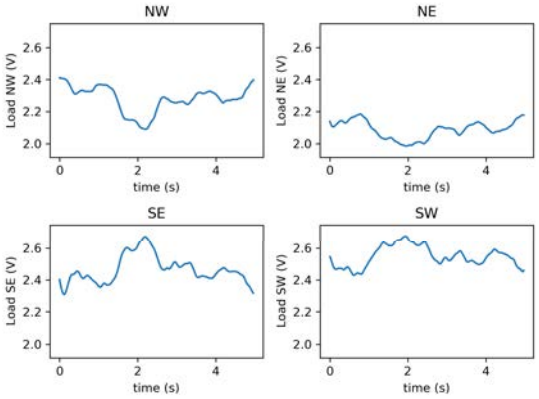

Figure 2: Tension measurement of the 4 load cells

Conclusion and Future Work

It is hoped this study will serve as a basis for the development of personal stabilometric balance monitoring platform which could better inform doctors on the health status of their more vulnerable patients, even if they are at home. Further research works could investigate the development of the stabilometric platform prototype. To make it more precise and to reduce the uncertainty of measurement, a stabilized power supply could be use. Filters can be also appropriate to reduce the signal noise. Moreover, the scale architecture could be rethink to take the forces in the scale pan plan and the torques in every direction into consideration. Future research works should also investigate machine learning as a tool to preventively identify the changes in the health status of vulnerable patients by detecting unusual variations in their longitudinal balance. To do so, collecting more data on different types of weighing will be required, with people of various ages and health conditions, in order to teach an AI how to detect abnormal changes in the longitudinal balance of the patients.

REFERENCES

[1] L. Calvet. *Health status and dependency of elderly people in institutions and at home.* Études et Résultats, DREES n 988, 2016.

[2] Dhouha Maatar. *Stabilometric signals analysis and biometric application.* Paris-Est University. 2013.

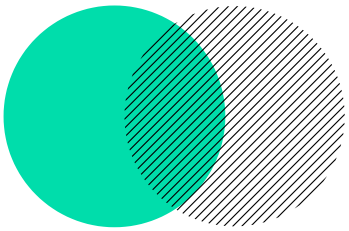

IMPROVEMENT OF BONDED INTERFACE BEHAVIOUR BY INTRODUCING CONTROLLED HETEROGENEITIES

NICOLAS CORTES - YACINE MANAL
FEDERICA DAGHIA

TER M1 2019-2020
FINAL DEFENCE OF RESEARCH PROJECTS
March 31, 2020, Cachan, France

école normale supérieure paris—saclay

TER M1 2019-2020
FINAL DEFENCE OF RESEARCH PROJECTS
March 31, 2020, Cachan, France

Improvement of bonded interface behaviour by introducing controlled heterogeneities

CORTES Nicolas*, MANAL Yacine*, DAGHIA Federica◇

* Département de Génie Mécanique
ENS Paris-Saclay
e-mail: nicolas.cortes@ens-paris-saclay.fr
e-mail: yacine.manal@ens-paris-saclay.fr

◇ Laboratoire de Mécanique et Technologies
ENS Paris-Saclay
e-mail: federica.daghia@ens-paris-saclay.fr

KEYWORDS: composite materials ; cracks propagation ; surface treatments ; fracture mechanics, finite element model.

ABSTRACT

In the aeronautic field, it has become necessary that structures and armatures materials become lighter in order to decrease the cost of travel fuel and thus considerably increase the autonomy of the travelling systems. Composite materials are an excellent compromise between mechanical and weight properties. In most cases, composites plates are fixed one to another with rivets which cause localised strain concentration but gluing the plates should allow a better strain distribution than the use of rivets.

Previous articles [1] have assessed and compared the impact of surface treatments in the holding of two glued plates under a mode I crack propagation load. The heterogeneities induced by laser irradiation surface treatments have been observed to cause the formation of glue filaments between the plates interfaces because of the differences of toughness. These filaments have been thought to increase the energy necessary to spread the crack but there has been no real study nor quantification of the impact of the heterogeneities.

The aim of our supervised research project was to assess the effect of interfaces of heterogeneous toughness and to create patterns in order to quantify the energy dissipated by the rupture of the glue in the first place and then maximise this energy.

Using the software Abaqus, we built several finite elements models composed of five distinct parts. Two plates of composite are separated from the glue by two interfaces. In order to make possible the propagation of a crack in these interfaces, they were made up with cohesive elements. In addition to have an elastic behaviour law, this kind of elements possess a special law of rupture so that each element can dissipate a predefined amount of energy before breaking.The heterogeneity was introduced by modifying the properties of specific areas. It means that we decreased the energy or the maximal stress of cohesive elements in these places. Several cases have been studied, in which the disposition and the characteristics of heterogeneities were modified.

The first models with uniform properties in the interfaces highlight the role of the energy and the maximal stress. When the energy is the same in the two interfaces but the maximal

stress is different, the crack begins in the interface with the lower maximal stress. It is the case even if the interface with the lower maximal stress possess an higher energy. Therefore, we can understand that the maximal stress is a key parameter of the crack initiation. When the maximal stress is the same in the two interfaces but the energy is different, the crack begins in the interface with the lower energy. However, the important thing to notice is that the lower the energy of the weaker interface is, the further the crack spreads. Hence, the energy directs the speed of the crack propagation.

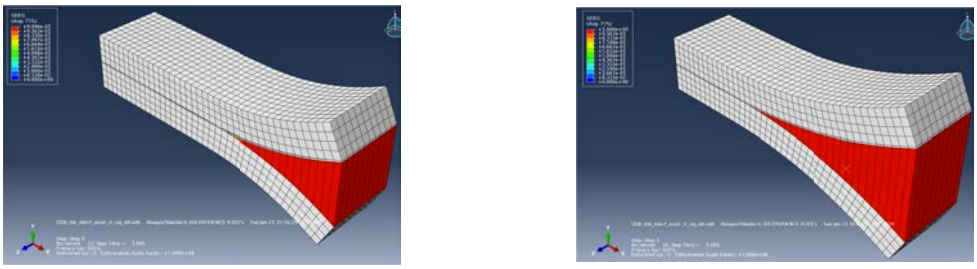

Figure 1: Damage of the interfaces : The interface energy is higher on the left than on the right

The last models where the strong and weak interfaces were alternated emphasised two potential manners to dissipate more energy. The first way is to cause the interface to break on a bigger surface for the same amount of energy. It means that the crack will spread less. It has been observed that when placing alternatively weak and strong interfaces face to face, it creates a glue filament. The second way is thus to create a glue filament which can enter its plastic domain and even break in order to absorb energy.

(a) Glue ligaments for heterogeneity in the width (b) Glue ligaments for heterogeneity in the length

Figure 2

Thus, our study presents potential phenomena that probably can be used to disperse more energy and hamper the propagation of cracks thanks to the introduction of controlled heterogeneities.

REFERENCES

[1] Ran Tao, Marco Alfano, Gilles Lubineau. Laser-based surface patterning of composite plates for improved secondary adhesive bonding. *Composites* **109**:84-94, 2018.

[2] Ran Tao, Marco Alfano, Gilles Lubineau. In situ analysis of interfacial damage in adhesively bonded composite joints subjected to various surface pretreatments. *Composites* **116**:216-223, 2019.

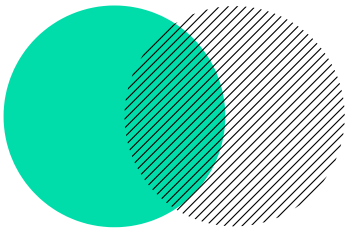

ANALYSIS AND MODELLING OF BIAXIAL DYNAMIC TESTS USING SLIDING SURFACES

BASTIEN SAUTY - YAN BARABINOT
BASTIEN DURAND

TER M1 2019-2020
FINAL DEFENCE OF RESEARCH PROJECTS
March 31, 2020, Cachan, France

école normale supérieure paris—saclay

Analysis and modelling of biaxial dynamic tests using sliding surfaces

Bastien Sauty*, Yan Barabinot*, Bastien Durand*

* Mechanical Engineering Department
Ecole Normale Supérieure Paris-Saclay
67 Avenue du Président Wilson, 94235 Cachan
e-mail: bastien.sauty@ens-paris-saclay.fr, yan.barabinot@ens-paris-saclay.fr,
bastien.durand@ens-cachan.fr

Keywords: biaxial compression; Hopkinson bar; digital image correlation; numerical simulation;

ABSTRACT

General Information

In the automotive and aeronautical industries, the mechanical behaviour of materials under shock stresses needs to be known by the designers in order to improve the systems during crashes. Hopkinson bars have initially been invented to carry out uniaxial compression dynamic tests on materials sample by reproducing the conditions of an impact. However, a material is rarely loaded along a single axis in real life and the complexity of the material behaviours thus made researchers turn to biaxial dynamic tests [1].

A mechanism with lubricated sliding surfaces has been developed by previous studies to execute a biaxial compression on a sample using a traditional Hopkinson bars setup. The mechanism transforms the axial load into two perpendicular loads both with half of the incoming amplitude. Strain is measured on the input and output bars with gauges, and the forces and displacements applied to the interfaces between the bars and the sample are identified through the theory of Hopkinson bars. The displacement field of the sample is obtained by high-speed imaging and by digital image correlation. Finally, the constitutive relation of the material is assessed through correlation of the measured load and the load calculated from the displacements [2].

Experiments show that the setup give acceptable results, but relies on the estimation of friction. To make the process more accurate, a new setup has to be developed to overcome the unknown friction.

Two solutions have thus been proposed : first to remove the friction by using a liquid as the angular transmission of the load. Second, to use a special hopkinson bars setup with one projectile but four incoming bars to measure strains after the sliding surfaces.

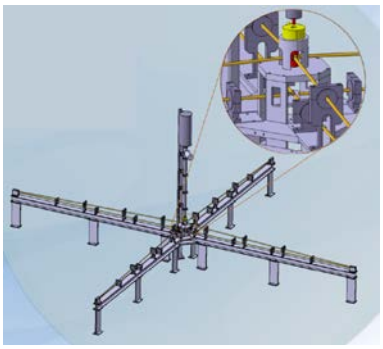

(a) setup with four incoming bars

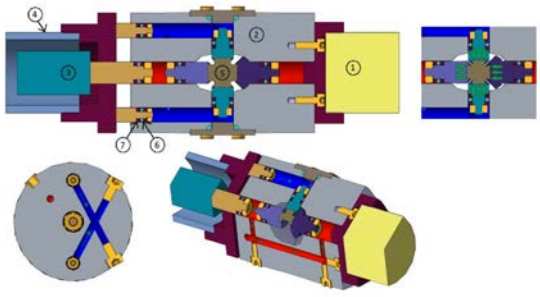

(b) setup with liquid

Studies

The presented study aims to characterize both mechanisms using the same aluminium sample whose geometry was designed to avoid buckling upon impact. Aluminium has the property to behave identically under stresses both statics or dynamics and mono-axial or bi-axial. First, a static test is

performed to determine the constitutive law of the material. Then, using the same sensors as in the first mechanism, the experimental load is compared to the load simulated with the constitutive relation and the experimental displacements.

Concerning the setup with liquid, the liquid in cavities is compressed and a stress is supposed to be applied on the sample when the compression wave make the output internal and the external bars move. Liquid friction and pressure loss can be neglected and because cavities have the same sections, transversal and longitudinal stress are theoretically the same. A traditional Hopkinson bars setup with three gauges on the input and both output bars must be used to carry out the test. Displacements and load applied on the sample are estimated thanks to the Hopkinson bar theory.

On the four bars setup, two gauges are required for each bar. The gauges are calibrated thanks to a static preload system. The bars are aligned in the same plane and point toward the center of the sample to avoid unsolicited movements and loads. This is achieved with a 3D printed part that rectifies the location of the bars and bends their extremities.

Results

The liquid setup proved to be unusable. The sample and the plugs that transfer the longitudinal pressure to the sample are too heavy regarding the input movement. Instead of rising the pressure in the longitudinal cavity, the liquid is transferred from one cavity to the other. It results in a shock between the sample and the body of the setup, which creates unsolicited and non-measurable loads.

The four bars setup showed to be much more satisfying. The figures 2a and 2b show the evolution of the loads in the bars of a same axis. The green and yellow curves are the experimentally measured loads and the purple one is the load calculated from the measured displacements. The results are conclusive and validate the use of the setup to estimate the constitutive law of a material under bi-axial compression load.

However the curve of load on the second axis show that the sample was not under a dynamic equilibrium. Further research must be carried out to understand the impact of the behaviour of the bars on the transmission of the waves and on the loading of the sample.

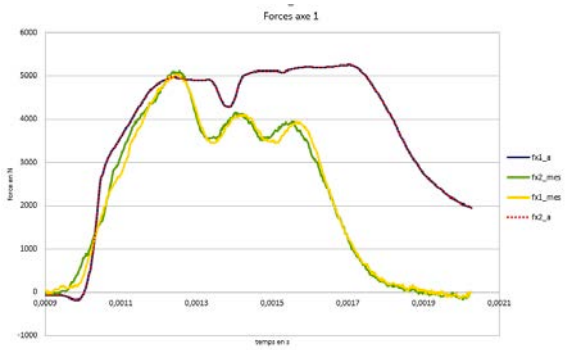

(a) results for the first axis

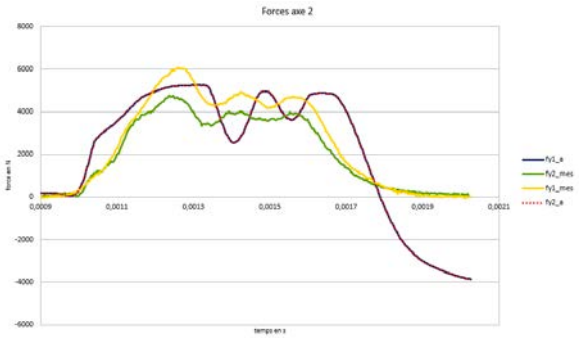

(b) results for the second axis

REFERENCES

[1] B.Durand, A.Zouari, H.Zhao Biaxial *Compression Tests on Hopkinson Bars*. 2018.

[2] P.Quillery, O.Hubert, B.Durand, H.Zhao *Experimental multiaxial dynamic behavior of nickel-titanium shape memory alloy*. 2019.

CORRECTING THE COLOR SHADE OF A SPECKLE TO IMPROVE STEREO-DIC MEASUREMENTS

XIHE GE - FLORIAN MAETZ
DAVID ETIEVANT - YANN QUINSAT

TER M1 2019-2020
FINAL DEFENCE OF RESEARCH PROJECTS
March 31, 2020, Cachan, France

école normale supérieure paris—saclay

Correcting the color shade of a speckle to improve stereo-DIC measurements

Xihe GE*, Florian MAETZ‡

Mechanical Engineering Department
ENS Paris Saclay
61, avenue du Président Wilson, F-94235 Cachan Cedex
*e-mail: xihe.ge@ens-paris-saclay.fr
‡e-mail: florian.maetz@ens-paris-saclay.fr

KEYWORDS : Stereo-DIC, Uniform gray level, Metrology

ABSTRACT

Nowadays, with increasing demand for the measurement of large-sized flexible parts, such as fuselage, stereo digital image correlation (stereo-DIC) is becoming a common practice for measurements. Stereo-DIC is an image analysis method that is based on the hypothesis of conservation of gray levels. For instance, it can be used to determine the position of points in space, thereby, allowing to measure the shape of an object remotely or its displacement. To be effective, the stereo-DIC needs a speckle on the object of interest, this speckle can be painted but more recent methods use a projector to project it on the surface. This allows to choose precisely what colors to project where and to quickly change, contrary to how long it takes to paint.

However, the projection is not perfect since a monochromatic projected image is not perceived as such by a camera, indeed the colors slightly fluctuate. This might lead to errors on the results of the stereo-DIC. This paper shows a process of calibration that aims to negate those fluctuations.
The process follows the next steps :

- First, a precalibration procedure was used to determine the relative positions of the objects, that is to say the camera and the projector related to the object of interest represented by its mesh. Those matrix were initialized by matching a set number of points (more than 6) between the picture, the projector and the mesh file. Then, an optimization process on those matrices was applied to improve the positioning of the different elements.
- The next step aims to map the response of the surface to different gray levels. In order to do so a set of data was gathered : Many pictures of different monochromatic projection were taken and averaged to attenuate noises caused by the environment.
- Once the data from the precedent points are available the corrected gray level to be projected can be computed on the nodes of the mesh. For each node the following tasks are done :
  - First, the coordinates of the nodes in the projector frame and in the picture frame were determined thanks to the matrices, so that there is a link between a point of the projector and a point of the picture.
  - Then, from the data gathered a linear interpolation was made as it can be seen in Figure 1a and the corrected gray level for one node was calculated and then stocked in a new picture giving a form of results that is close to what is represented in Figure 1b.

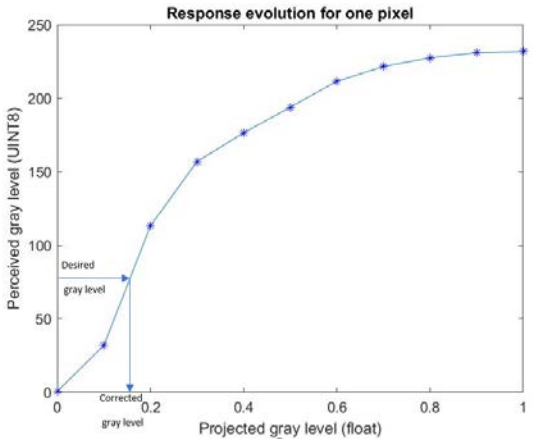

(a) Correction process for one pixel

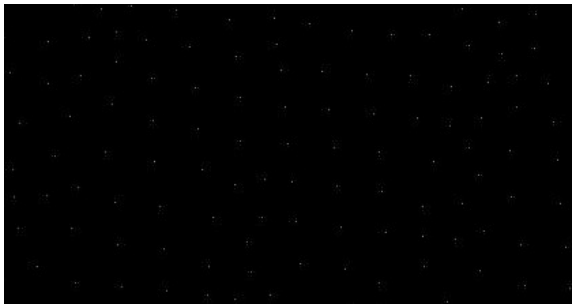

(b) Picture corrected on the nodes

FIGURE 1: Correction on the nodes

— The picture to be projected only had the pixels corresponding to the nodes corrected, to correct all pixels of the projected picture an interpolation was made between the pixels of the nodes resulting in the corrected picture to be projected as it can be seen in Figure 2.

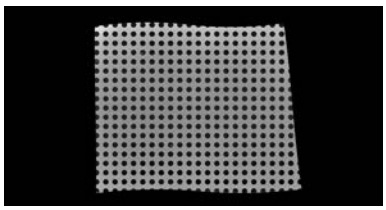

FIGURE 2: Example of a full correction

To evaluate the utility of the process we compared the distribution of the gray levels before and after the correction of a projection of a monochromatic picture. We succeeded in reducing the span of gray levels perceived by around 50 % as the Figure **??** shows. On this figure the histogram of gray levels perceived by the camera is represented, with a red color for corrected picture and blue for non-corrected ones. However this result can still be improve since there was an issue with the precalibration procedure that resulted in errors on the matrices.

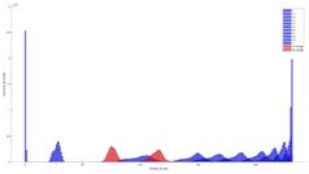

FIGURE 3: Before and after correction of monochromatic picture

Further tests could be performed by testing the stereo-DIC after the correction, since stereo-DIC uses more than one camera a correction for each camera should be computed. A way to sum those correction would be to average them. Another point is that the projected image is colorized and not in shades of gray so we could improve the whole process to correct not only the gray level but more precisely the color projected thanks to the control of the RGB values of a pixel.

NUMERICAL INVESTIGATION OF THE ROUGHNESS EFFECT ON PLASTIC STRAIN LOCALIZATION IN THREE-DIMENSIONAL POLYCRYSTALLINE AGGREGATES

MAXIME LALANDE - JULIEN LANGLOIS
YOANN GUILHEM

TER M1 2019-2020
FINAL DEFENCE OF RESEARCH PROJECTS
March 31, 2020, Cachan, France

école normale supérieure paris—saclay

TER M1 2019-2020
FINAL DEFENCE OF RESEARCH PROJECTS
March 31, 2020, Cachan, France

Numerical investigation of the roughness effect on plastic strain localization in three-dimensional polycrystalline aggregates

M. Lalande*, J. Langlois†, Y. Guilhem◇

Department of Mechanical Engineering
Ecole Normale Supérieure Paris-Saclay
61, avenue du président Wilson 94230 Cachan, France
e-mail: {*maxime.lalande, †julien.langlois, ◇yoann.guilhem}@ens-paris-saclay.fr

KEYWORDS: microstructure; mechanical behaviour of materials; plasticity; fracture mechanics; finite element analysis

ABSTRACT

Micro-cracks in early stages with a length of the order of a few grains are a determining factor in the fatigue life of polycrystals. Various studies relying on both experimental observations and numerical analysis have shown the influence of microstructure on short crack generations: grain boundaries and orientations, inclusions and persistent slip bands play a very important role in the incubation phase under high cycle fatigue conditions [1].As a result of industrial processes, a surface state is also frequently involved that can be either beneficial or detrimental for the materials. The impact of this surface state is discussed in several articles but due to the large number of parameters that govern surface finishing - including roughness, residual stresses and local work hardening - no result allows to fully characterise its competition with the microstructure in the localisation phenomena [2].

The aim of this research project is to better understand the influence of some specific parameters to surface roughness and the load orientation on local stress and strain fields in polycrystalline aggregates. The study is part of research aimed to:

1. determine the conditions under which the surface state is predominant over the effects of microstructure,
2. deduce a more reliable fatigue criterion based on the results referred to in [1].

To evaluate the local mechanical fields, we used the Finite Element Crystal Plasticity Method (FECP) on a three-dimensional 316L stainless steel aggregate as shown in Figure 1 and made of shaped-oriented grains generated with Neper. Evolution law was based on the Méric-Cailletaud's crystal plasticity model [3]. The aggregate was subject to a loading cycle (0° orientation corresponding to the direction of the striations) with noisy sine-like roughness on its free surface. Depending on a computational routine, we generated the fields for three different micro-structural configurations by varying the following parameters: arithmetical mean deviation (R_a), wavelength (λ), phase of the roughness (φ) and load orientation.

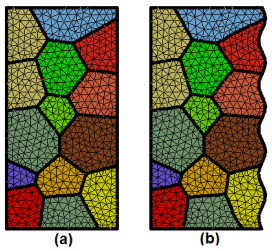

Figure 1: Polycrystalline aggregate generated by Neper in the flat (a) and rough (b) cases.

To compare the results obtained on rough meshes to the reference flat case, we provide the Induced Roughness-Perturbation Indicator (IRPI) which characterises the influence of the roughness on the local mechanical fields:

$$\mathrm{IRPI}(X, k_r) = \frac{1}{N_{\mathrm{IP}}} \sum_{i=1}^{N_{\mathrm{IP}}} \left| \frac{X\,(k_r) - X\,(k_r = 0)}{X\,(k_r = 0)} \right|$$

with X a generic local variable, k_r a roughness configuration and N_{IP} the total number of integration points. This study is exclusively focused on $X = \gamma_{\mathrm{cum}}$ the sum of accumulated plastic slip on all slip systems.

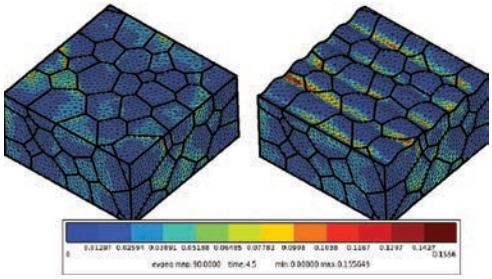

Figure 2: Plastic strain localisation using the FECP method in flat and rough cases.

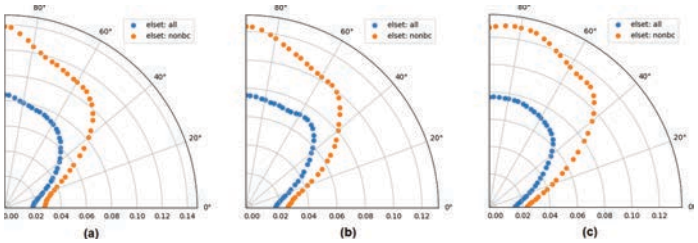

Figure 3: Evolution of IRPI according to the loading angle with consideration of boundary conditions for three polycrystalline configurations.

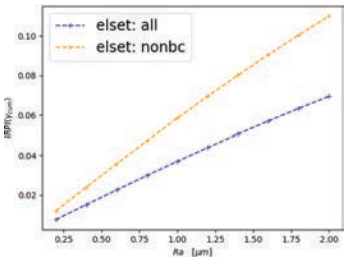

Figure 4: Evolution of IRPI as a function of R_a.

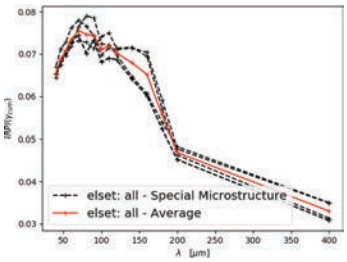

Figure 5: Evolution of the IRPI as a function of the roughness wavelength for different configurations and average.

Figure 2 shows the stress locations after post-processing finite element calculation results. Unlike previous conclusions in [2] which studied the impact of striation direction for fixed loading and observed a maximum IRPI(γ_{cum}) for a roughness direction of 45°, the loading direction here has a significant impact on IRPI until 50° and tends towards a constant from 50° to 90°, as illustrated in Figure 3. Above 50°, striations are stressed in opening and sliding failure modes that are independent of the microstructure and could explain IRPI's constant. Results also show an approximate ratio of 5 between the IRPI at 90° and 0° as opposed to Dassonville's study which presented a ratio of 2. The curve shape is independent from the considered polycrystalline configuration, which motivates the use of the Induced Roughness-Perturbation Indicator.

The study also points out that wavelength and R_a contribute to roughness impact on localisation phenomena. Trends for R_a influence are consistent with literature results: mean deviation being an image of the roughness amplitude, the quasi-linear relation observed in Figure 4 reflects a stress concentration in the notched areas. The interpretation for the wavelength in figure 5 requires more careful examination. If the decrease for high λ values can simply be explained (roughness tends towards a flat case), variations below 150 µm could have different explanations but appear to be due to the localisation area becoming too small (reduction of the surface in the roughness hollows).

The calculation routine developed in this study facilitates the automation of the problem setting and allows for effective post-processing. In comparison with previous works, results on the R_a influence on the localisation phenomena support the validity of the conclusions. This research highlights the impact of loading orientation in relation to roughness direction, but has yet to be compared to the isotropic case. Short wavelength influence requires further refinement of the mesh, which will increase computation time. Further work could focus on calculations on the phase and thus will enable to deduce the role of the main roughness parameters (λ, R_a, φ) on the generation of micro-cracks.

REFERENCES

[1] S. Basseville, G. Cailletaud, T. Ghidossi, Y. Guilhem, E. Lacoste, H. Proudhon, L. Signor, P. Villechaise. Numerical analysis on the local mechanical fields in polycrystalline 316LN stainless steel under cyclic fatigue loading : Comparison with experimental results. *Elsevier* **Vol 696** : pp 122-136, 2017.

[2] T. Dassonville. Numerical study of the influence of microstructural parameters and roughness on fatigue cracks appearance in polycrystals. *Rapport de stage*. 2017

[3] L. Méric, G. Cailletaud. *J. of Engng. Mat. Technol.* **Vol 113** : pp 171-182, 1991.

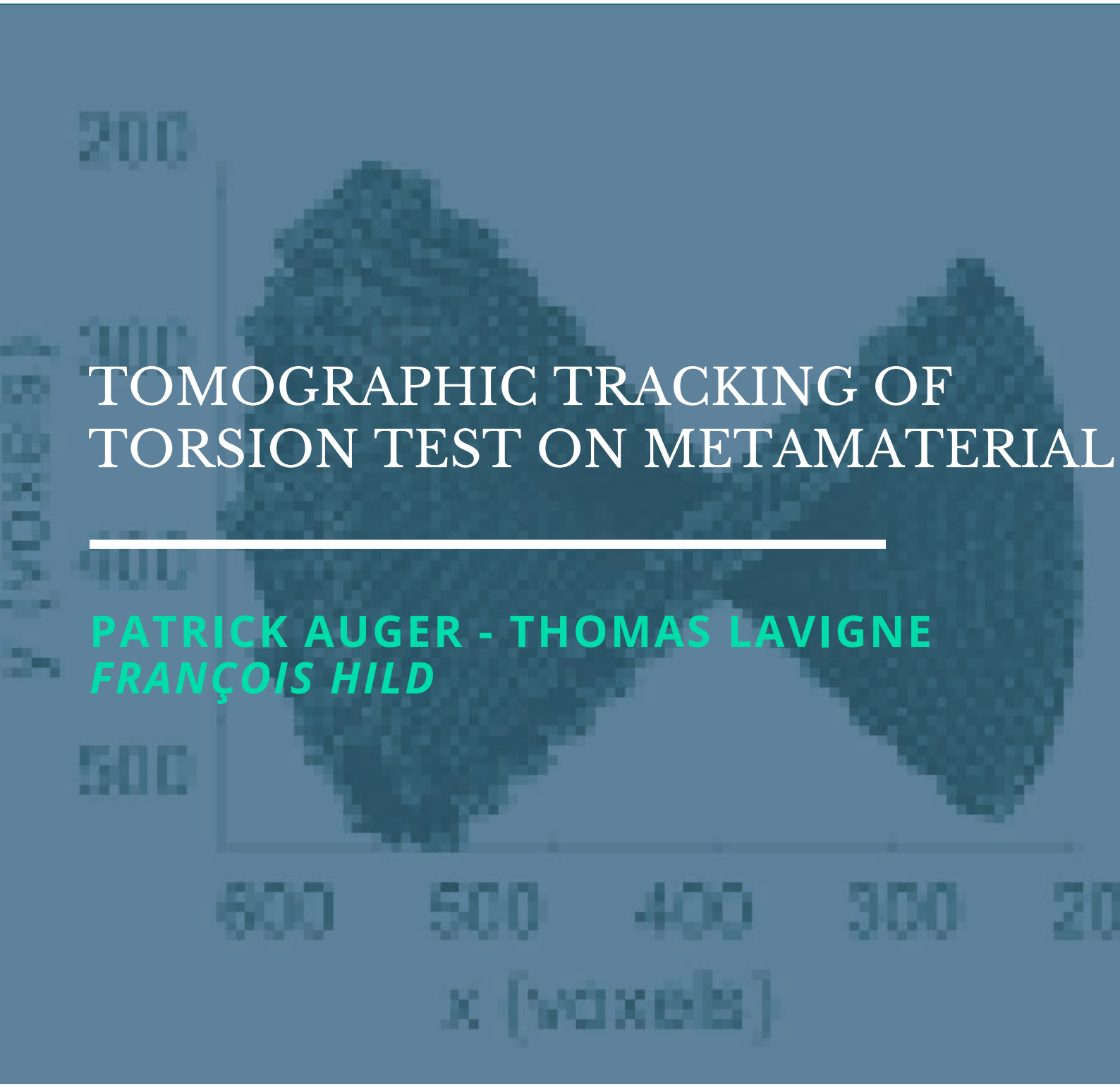

TOMOGRAPHIC TRACKING OF TORSION TEST ON METAMATERIAL

PATRICK AUGER - THOMAS LAVIGNE
FRANÇOIS HILD

TER M1 2019-2020
FINAL DEFENCE OF RESEARCH PROJECTS
March 31, 2020, Cachan, France

école normale supérieure paris—saclay

TER M1 2019-2020
FINAL DEFENCE OF RESEARCH PROJECTS
March 31, 2020, Cachan, France

Tomographic Tracking Of Torsion Test On Metamaterial

P. Auger*, T. Lavigne*, F. Hild◇

École normale supérieure Paris-Saclay
61 avenue du Président Wilson, 94235 Cachan Cdex, France
* Department of Mechanical Engineering
e-mail:{patrick.auger,thomas.lavigne}@ens-paris-saclay.fr
◇LMT - Laboratoire de Mécanique et Technologie
e-mail: francois.hild@ens-paris-saclay.fr

KEYWORDS: Digital Volume Correlation; Poynting Effect; Tomography; Torsion Test.

ABSTRACT

Metamaterials are often used for their peculiar mechanical properties [1]. However, few studies were conducted on a 3D printed pantograph. This project aims at performing an in situ torsion test in a lab tomograph. The acquired scans are used to measure displacement fields via digital volume correlation. The final goal is to analyze the deformation mechanisms of an Inconel 718 (i.e. nickel-chromium superalloy) pantograph and to rationalize a potential Poynting effect [1].

Methods The torsion test was monitored using micro-computed tomography. Such imaging technique is non-intrusive and provides 3D images of the sample. The torsion torque was applied by two angular actuators of the in situ testing machine, both controlled in angular position. The levels of torque and axial force were regularly recorded. The test was conducted until reaching an angular amplitude of $\theta = 180°$ between the bottom and the top platens (Figure 1). A last step consisted in getting back to the initial angular position.

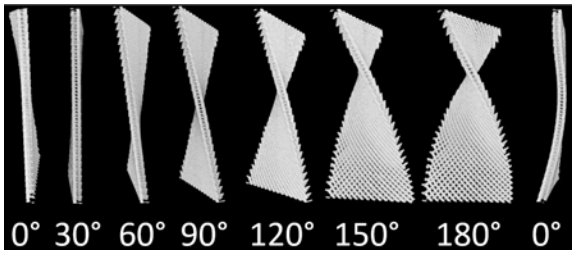

Figure 1: 3D renderings of the tested sample for different angular amplitudes θ in torsion

The region of interest covered $70 \times 70 \times 50\text{mm}^3$ with a 50 µm resolution. The series of radiographs (i.e. sinograms) were used to reconstruct 3D images of the sample (Figure 1). The displacement fields were then measured using Digital Volume Correlation (DVC). As the initial sample was already deformed by the printing method, an additional DVC analysis was conducted between the image of the nominal geometry and that of the printed shape, to backtrack the mesh that was constructed on the nominal geometry. DVC was then run incrementally on the different deformed configurations (Figure 1), and then directly, both with mechanical regularization [2].

Results An axial force was observed during the torsion test (Figure 2(b)), which is the so-called Poynting effect [1]. From Figure 2, three different regimes are observed: first, a

quasi-linear part ($\theta \in [0°, 30°]$). Then, the torque increases non-linearly while the force still increases quasi-linearly but with a lower slope ($\theta \in [30°, 70°]$) due to the plastic behaviour of the alloy (Figure 1). The force reaches a maximum at $\theta \approx 70°$, and slowly decreases quasi-linearly while the torque tends to saturate ($\theta \in [70°, 180°]$). These three different regimes illustrate the existence of both direct and reverse Poynting effects during the torsion test.

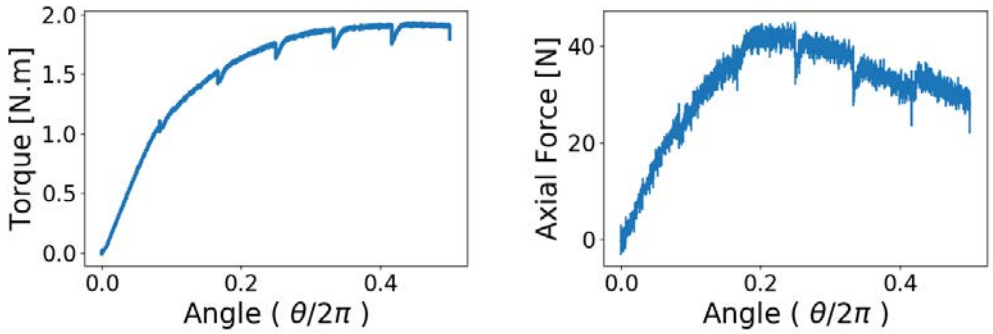

(a) (b)

Figure 2: Torsion torque (left) and resultant force (right) during the loading part of the test

The DVC results (Figure 3) highlight the existence of these three regimes. Firstly, the shear strains ϵ_{xy} are evenly distributed in the whole pantograph (Figure 3(a)). Then, after the third scan (i.e. $\theta = 90°$), the strains begin to concentrate around the hinges (Figure 3(b)). Finally, the strains are prevailing in the hinges (Figure 3(c)).

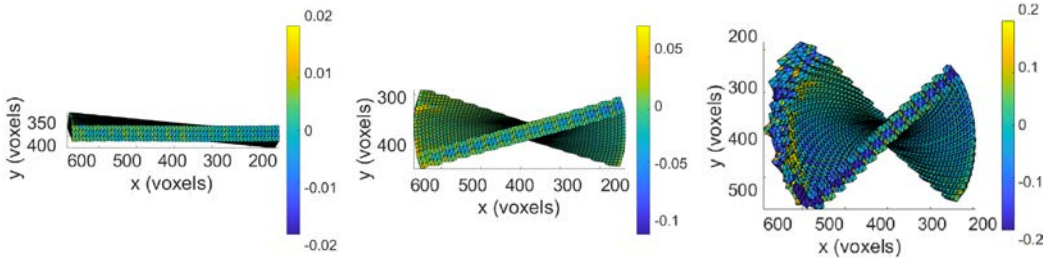

(a) $\theta = 30°$ (b) $\theta = 90°$ (c) $\theta = 180°$

Figure 3: Strain ϵ_{xy} fields for three different deformed configurations

References

[1] A. Misra, T. Lekszycki, I. Giorgio, G. Ganzosch, W. H. Müller, and F. dell'Isola, "Pantographic metamaterials show atypical poynting effect reversal," *Mechanics Research Communications*, vol. 89, pp. 6–10, 2018.

[2] Z. Tomičević, F. Hild, and S. Roux, "Mechanics-aided digital image correlation," *Journal of Strain Analysis for Engineering Design*, vol. 48, pp. 330–343, 2013.

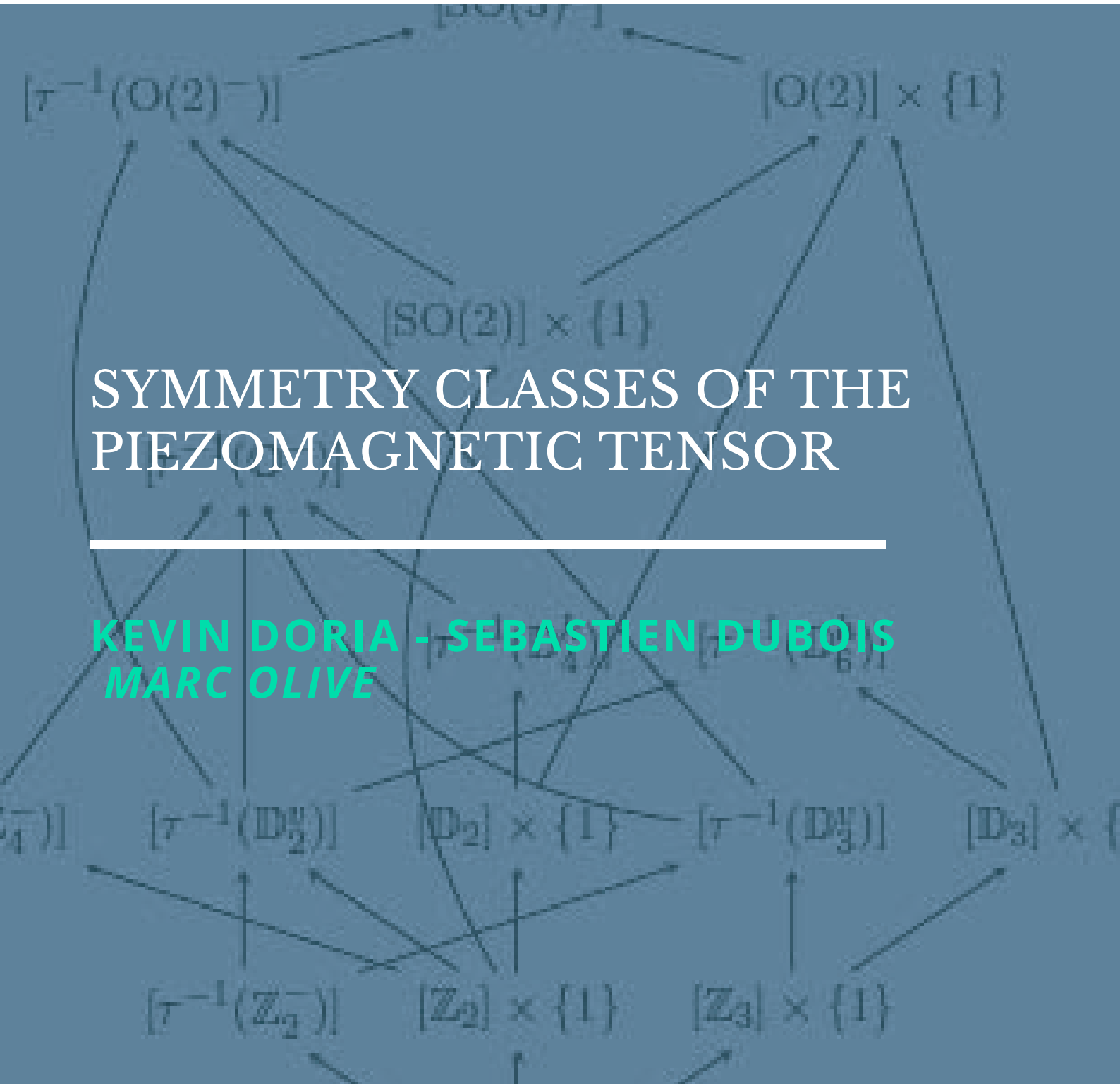

SYMMETRY CLASSES OF THE PIEZOMAGNETIC TENSOR

KEVIN DORIA - SEBASTIEN DUBOIS
MARC OLIVE

TER M1 2019-2020
FINAL DEFENCE OF RESEARCH PROJECTS
March 31, 2020, Cachan, France

école normale supérieure paris—saclay

TER M1 2019-2020
FINAL DEFENCE OF RESEARCH PROJECTS
March 31, 2020, Cachan, France

Symmetry Classes of the Piezomagnetic Tensor

Kévin Doria[1], Sébastien Dubois[1], Marc Olive[2]

[1] Mechanical Engineering Department
Université Paris-Saclay
61 Avenue du President Wilson, 94230 Cachan
e-mail: kevin.doria@ens-paris-saclay.fr / sebastien.dubois@ens-paris-saclay.fr

[2] LMT Laboratory
Université Paris-Saclay
61 Avenue du President Wilson, 94230 Cachan
e-mail: marc.olive@ens-cachan.fr

KEYWORDS: Piezomagnetism; Anisotropy; Symmetry Class

ABSTRACT

Since Forte–Vianello's work [1], it has been known that there are only 8 kinds of anisotropy in elasticity and 16 types in piezoelectricity [2]. They are defined to be symmetry classes. However, the number of possible anisotropies remains to be clearly stated in the case of piezomagnetism [3]. In the linear theory of piezomagnetism, there is a relation between the (infinitesimal) strain tensor ε and the magnetization pseudo–vector $\mathbf{m}$. At vanishing stress and around initial magnetization $\mathbf{m}^0$, this writes :

$$\varepsilon = \mathbf{\Pi}(\mathbf{m} - \mathbf{m}^0), \quad \varepsilon_{ij} = \Pi_{ijk}(m_k - m_k^0), \quad \Pi_{ijk} = \Pi_{jik}$$

where $\mathbf{\Pi}$ is the piezomagnetic pseudo–tensor. The vector space of piezomagnetic tensors is called $\mathbb{M}$agn. A significant specificity of piezomagnetism is that the group O(3) of orthogonal transformations is not the only one to be considered. There is also a time-reversal $t \mapsto \pm t$ transformation [4], so that a spatio–temporal orientation change is modelled by elements of $\mathrm{O}(3)^\mu := \mathrm{O}(3) \times \{+1; -1\}$. More precisely, take some material with a piezomagnetic tensor $\mathbf{\Pi}$ defined in some orientation of time-space, then for any $(g, \delta) \in \mathrm{O}(3)^\mu$, the piezomagnetic tensor

$$\overline{\mathbf{\Pi}}_{ijk} := ((g, \delta) \star \mathbf{\Pi})_{ijk} = \delta \det(g) g_{ip} g_{jq} g_{kr} \mathbf{\Pi}_{pqr} \tag{1}$$

is associated to the same material.

In the linear group representation theory (1) translates into a representation of $\mathrm{O}(3)^\mu$ on $\mathbb{M}$agn. With this approach, the initial problem regarding anisotropy is equivalent to the effective determination of the symmetry classes for the piezomagnetic tensor. A definition of the anisotropy that does not depend on the orientation of the material under study is thus obtained. The study was then reduced to the determination of the symmetry classes of the piezoelectric tensor space ($\mathbb{P}$iez) under the action of O(3) as :

- $\mathrm{O}(3)^\mu$ representation can be reduced to $\mathrm{SO}(3)^\mu$
- $\mathrm{SO}(3)^\mu$ and O(3) are isomorphic, via $\tau : (g, \delta) \in \mathrm{SO}(3)^\mu \mapsto \delta g \in \mathrm{O}(3)$

The symmetry classes of $\mathbb{P}$iez have been obtained by Olive [2] via a harmonic decompo -sition, achieved with an extension of the Clebsch-Gordan formula for instance. This leads to an isomorphism

$$\mathbb{P}\mathrm{iez} \simeq \mathbb{H}^3 \oplus \mathbb{H}^{-2} \oplus \mathbb{H}^1 \oplus \mathbb{H}^1$$

With $\mathbb{H}^n$ being the space of n–th order harmonic tensor (totally symmetric and traceless) and $\mathbb{H}^{-2}$ the space of second order symmetric pseudo–tensors. This way, 16 symmetry classes are obtained for $\mathbb{P}$iez. The isomorphism τ is finally used to transpose these symmetry classes for the piezomagnetism tensors. We have thus determined that there are 16 types of anisotropy in piezomagnetism and our work leads to the following theorem.

Theorem 1 $\mathbb{M}$agn *has 16 symmetry classes, summarised in Figure 1 and listed below:*

$$\{\,[1\times\{1\}], [\mathbb{Z}_2\times\{1\}], [\mathbb{Z}_3\times\{1\}], [\mathbb{D}_2\times\{1\}], [\mathbb{D}_3\times\{1\}], [\mathrm{SO}(2)\times\{1\}], [\mathrm{O}(2)\times\{1\}], [\tau^{-1}(\mathbb{Z}_2^-)],$$

$$[\tau^{-1}(\mathbb{Z}_4^-)], [\tau^{-1}(\mathbb{D}_2^v)], [\tau^{-1}(\mathbb{D}_3^v)], [\tau^{-1}(\mathbb{D}_4^h)], [\tau^{-1}(\mathbb{D}_6^h)], [\tau^{-1}(\mathbb{O}^-)], [\tau^{-1}(\mathrm{O}(2)^-)], [\mathrm{SO}(3)^\mu]\}$$

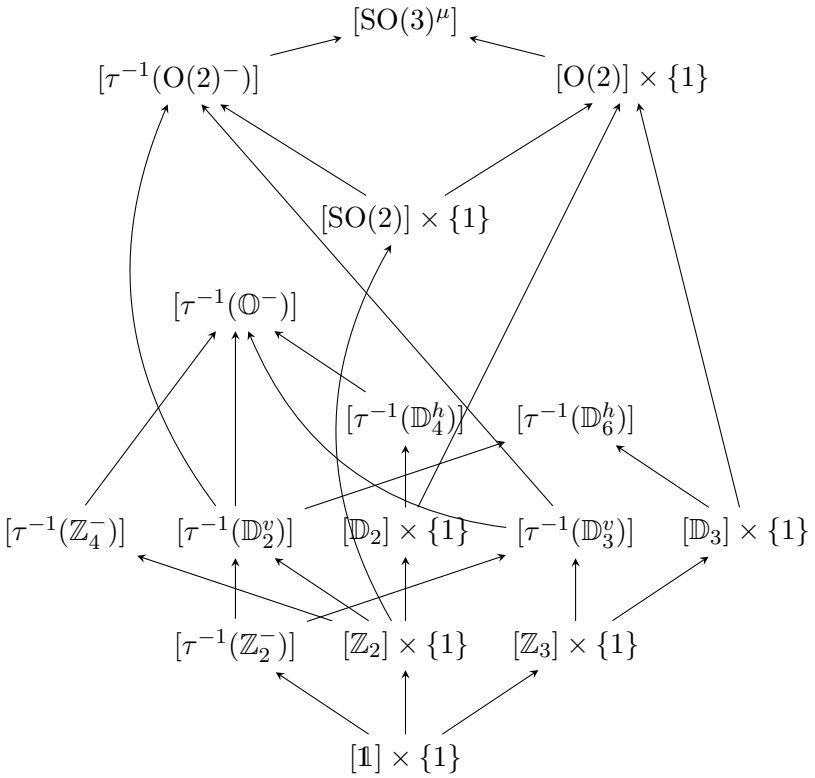

Figure 1: Symmetry classes for $\mathbb{M}$agn

REFERENCES

[1] Sandra Forte & Maurizio Vianello. *Symmetry Classes for Elasticity Tensors*. Journal Of Elasticity **43,** 81–108, 1996.

[2] Marc Olive. *Effective computation of* SO(3) *and* O(3) *linear representations symmetry classes*. 2017.

[3] Thibaut Weller & Giuseppe Geymonat *Piezomagnetic tensors symmetries: an unifying tentative approach*. Configurational Mechanics, *A. A. Balkema Publishers*, 13p., 2004. 2013.

[4] E. Kiral & A.Cemal Eringen, *Constitutive Equations of Nonlinear Electromagnetic-Elastic Crystals*, Springer New-York, 1990.

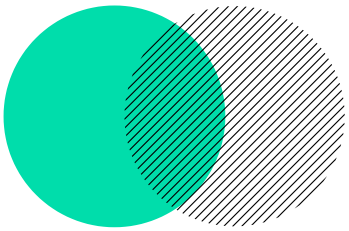

EXOTIC BEHAVIOUR AND RICH BOUNDARY CONDITIONS

MARTIN HOUOT - QUENTIN LANÇON
MARTIN PONCELET

TER M1 2019-2020
FINAL DEFENCE OF RESEARCH PROJECTS
March 31, 2020, Cachan, France

école normale supérieure paris—saclay

TER M1 2019-2020
FINAL DEFENCE OF RESEARCH PROJECTS
March 31, 2020, Cachan, France

Exotic behaviour and rich boundary conditions

M. Houot*, Q. Lançon†, M. Poncelet◇

* Mechanical Engineering
École Normale Supérieure Paris-Saclay
e-mail: martin.houot@ens-paris-saclay.fr and quentin.lancon@ens-paris-saclay.fr

◇ Laboratoire de Mécanique et Technologie
École Normale Supérieure Paris-Saclay
e-mail: martin.poncelet@ens-paris-saclay.fr

KEYWORDS: architectured materials; second gradient; homogenization, experimental testing

ABSTRACT

General Information

Over the course of this research project, the focus was on the characterization of heterogeneous materials. When a material is not homogeneous but complex as architectured materials are, the study of their behaviour is harder, since the materials do not behave according to Cauchy's theory of elasticity, when the stress is directly linked to the deformation [1]. It is in this specific situation, where terms from superior orders appear, terms from the second gradient of displacement, which will be the focus of this study.

The problematics of this research subject were also the main interest of other researchers, including P. Seppecher and H. Abdoul Anziz [2, 3], who worked on building a complex periodic structure, which comported no first order stiffness, but only superior orders ones (see Figure 1). In his work he proved theoretically this behaviour, yet, he did not succeed in confirming this theory with experimental results.

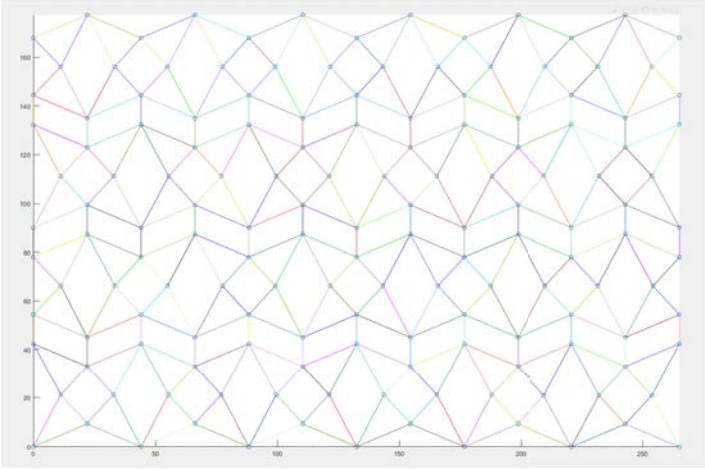

Figure 1: The theoretical structure

Our project

Through this year, we have worked to valid or not his theory with experimental results. To do this, our objective was to conceive an innovative tensile test on this architectured material, enabling to obtain concrete observations of the structure's behaviour, since the ordinary tensile test does not permit to observe second gradient behaviour.

The first stage of the project, was to determine how to produce a test specimen consistent with the theoretical structure. It needed to have a bending energy as low as possible in order to leave only the second gradient energy. Our main idea to do that was to use flexible joints inside the architecture, acting as pivoting links (see Figure 2).

In a second time, we had to determine the optimal manufacturing process for this specimen, thus, we tried several processes and our final choice was to use water jet cutting to obtain a precise and a one-piece structure (see Figure 2).

After finding a way to apply the mechanical stress during the test (see the drilled holes on Figure 2), we were able to perform the final test. By using an image correlation algorithm specific for pantographs, the effective behaviour of the structure could finally be highlighted.

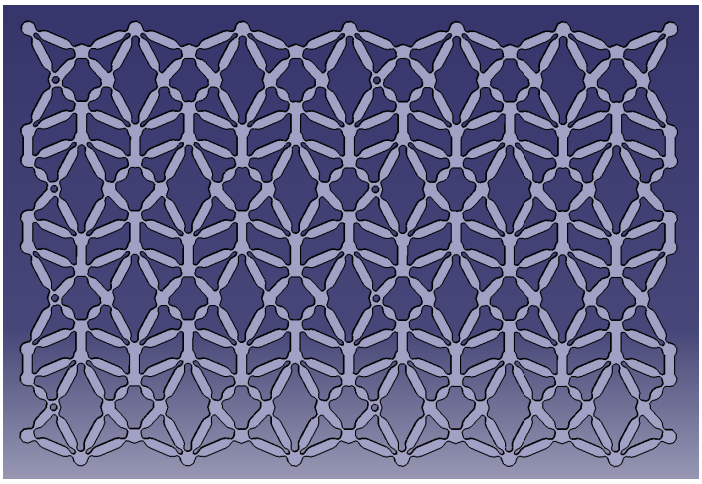

Figure 2: Our experimental structure

REFERENCES

[1] M. Poncelet, A. Somera, C. Morel, C. Jailin, N. Auffray. *An experimental evidence of the failure of Cauchy elasticity for the overall modeling of a non-centro-symmetric lattice under static loading*. International Journal of Solids and Structures, 2018.

[2] P. Seppecher, H. Abdoul Anziz. *Homogenization of periodic graph-based elastic structures*. Journal de l'École polytechnique, 2017.

[3] H. Abdoul Anziz. *Homogénéisation de composites élastiques périodiques à fort contraste. Conception de métamatériaux de second gradient*. Institut de Mathématiques de Toulon, 2018.

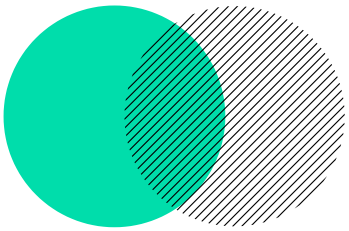

QUALITY ASSESSEMENT OF THE LAYERING FOR THE LASER POWDER BED FUSION PROCESS

VIRGILE BATTO - EMILE SIBOULET
YANN QUINSAT - CHRISTOPHE TOURNIER

TER M1 2019-2020
FINAL DEFENCE OF RESEARCH PROJECTS
March 31, 2020, Cachan, France

école normale supérieure paris—saclay

TER M1 2019-2020
FINAL DEFENCE OF RESEARCH PROJECTS
March 31, 2020, Cachan, France

Quality assessement of the layering for the laser powder bed fusion process

Virgile BATTO*, Émile SIBOULET*,
Yann QUINSAT◇, Christophe TOURNIER◇

* Department of Mechanical Engineering
École Normale Supérieure Paris-Saclay
61, avenue du President Wilson,
94230 Cachan
virgile.batto@ens-paris-saclay.fr
emile.siboulet@ens-paris-saclay.fr

◇ LURPA Laboratory
University of Paris-Saclay
61 Avenue du President Wilson,
94230 Cachan
yann.quinsat@ens-paris-saclay.fr
christophe.tournier@ens-paris-saclay.fr

KEYWORDS: Laser power bed fusion ; powder layering ; fine-tuning.

ABSTRACT

General Information

Laser powder bed fusion(LPBF) manufacturing is one of the fastest ways to prototype heavy-duty components. The main problem encountered during the manufacturing of a new component is the lack of repeatability which can comes from the inaccuracy of the layering device. Precedent studies have tried to implement some sensors to detect flaws in the layering technique and succeeded to show irregularities on layers but they did not succeed in getting information on the printer itself[1],[2]. Another method to assess the quality of layering needs to be developed.

Objectives

In our study we focus on the layering of the bed powder inside an AddUp printer who use a roller to dispatch the powder. In order to measure the height of the layered powder we have implemented an optical sensor, which can detect 1μm defect, on the spreading cart. Our main goal is to setup a turnkey experience that can be implemented on multiple 3D printers to accelerate prototyping on new equipment.

Experimentation

The first part of the project was to design parts(figure 1) to measure the bed powder. Multiple issues as to be faced, the printer must remain inert during printing, all the equipment that come close from the machine need to resist the metallic dust (figure 2) .

After validating the experimental setup, we test in with rectified plans to detect flaws in our conception.

Figure 1: Sensor support

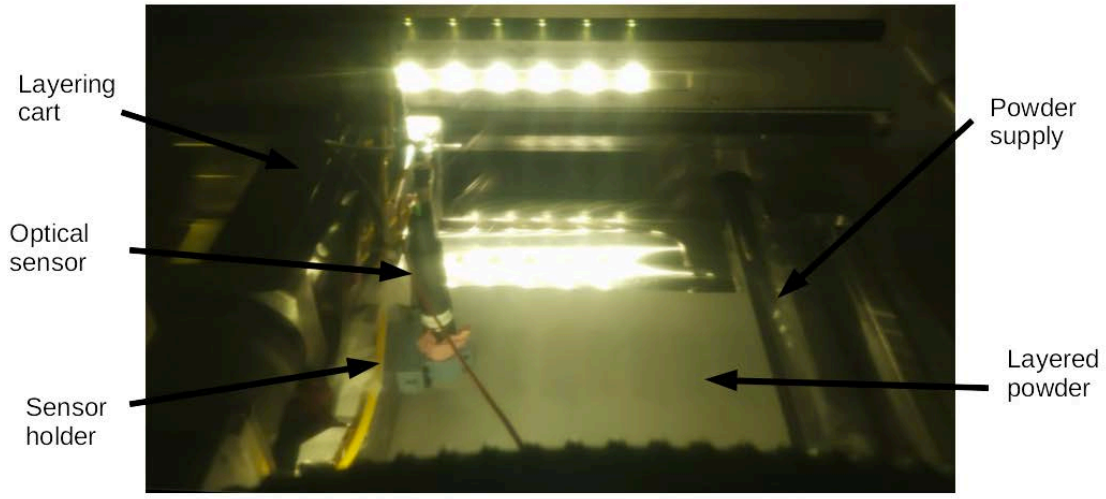

Figure 2: Experimental setup

Results

The analyses of the different geometric defects make us able to understand what causes a bad straightness of a powder bed. The result show that we can differentiate some defects which come from the general structure of the printer and some other from the roller. In our cases the roller was the main source of problems.

Conclusion

Our method could be used to determine what is the printing problems on these printers. To validate the method the same study has to be conducted on other LPBF printers. The study was only focusing on the layering, to validate the full process another study on the fusion needs to be conducted. A further analysis is needed to link the defect of the powder bed and the defect in the final product.

REFERENCES

[1] A.R. Nassar B. T. Hall S.W. Brown C.J. Dickman B. K. Foster, E. W. Reutzel1. Optical, layerwise monitoring of powder bed fusion.

[2] R. Goodridge R. Leach N. Southon, P. Stavroulakis. In-process measurement and monitoring of a polymer laser sintering powder bed with fringe projection. *Materials & Design 157*, 2018.

DEVELOPMENT OF SIMPLE AND PRACTICAL DIGITAL TOOLS FOR IN-SITU CONTROL OF THE ADDITIVE LPBF MANUFACTURING PROCESS

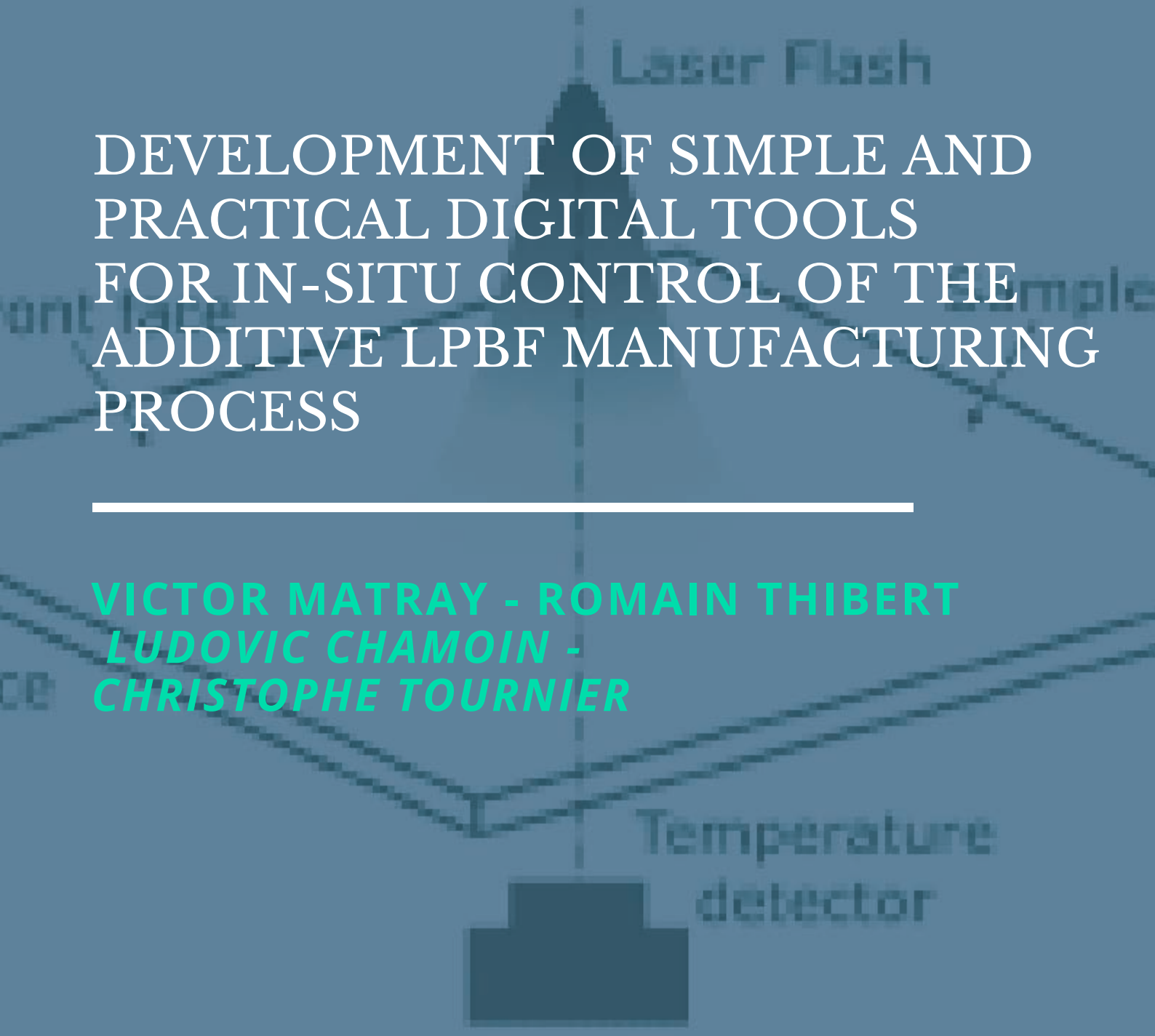

VICTOR MATRAY - ROMAIN THIBERT
LUDOVIC CHAMOIN - CHRISTOPHE TOURNIER

TER M1 2019-2020
FINAL DEFENCE OF RESEARCH PROJECTS
March 31, 2020, Cachan, France

école normale supérieure paris—saclay

Development of simple and practical digital tools for in-situ control of the additive LPBF manufacturing process

Victor Matray*, Romain Thibert*, Ludovic Chamoin†, Christophe Tournier◇

* Department of Mechanical Engineering
École normale supérieure Paris-Saclay
4 Avenue des Sciences, 91190 Gif-sur-Yvette

◇Université Paris-Saclay
ENS Paris-Saclay
LURPA
4 Avenue des Sciences, 91190 Gif-sur-Yvette,
France

†Université Paris-Saclay
ENS Paris-Saclay
LMT
4 Avenue des Sciences, 91190 Gif-sur-Yvette,
France

E-MAIL : { victor.matray ; romain.thibert ; ludovic.chamoin ; christophe.tournier } @ens-paris-saclay.fr

KEYWORDS: Additive Manufacturing; LPBF process; Residual Stresses

ABSTRACT

Context and Objectives

Additive Manufacturing has become used at large scales in industry and problematics of consistency and feasibility have risen. In the Laser Powder Bed Fusion (LPBF) process, in which metallic powders are melted into a solid piece, a major issue is that during cooling phases the material retracts and thus creates internal residual stresses in the final part. The challenge is then to determine the final impact of residual stresses caused by the geometry of the part and the laser strategy used.

Methodology

Previous works [4] have developed analytical models to assess residual stresses during LPBF processes at a high computing cost for a while print. Fergani et al. Fergani *et al.*[1] have built a method based on thermal cycles using a model previously developed to evaluate residual stresses under cyclic elasto-plastic hertzian contact [3].
To compute a residual stress map, a temperature map has to be established, this is obtained with the FLASH technique developed in [2]. This analytical model simulates the thermal effect of the laser trajectory as a succession of elementary pulses (Figure 1), which allows reasonable simulation times. The aim of this work is to obtain an analytical model of residual stresses during LPBF process based on the laser path during the process and to compare scanning strategies through the stress generated in the parts.

Furthermore, the interest of the targeted purely analytical model, contrary to commercial codes based exclusively on finite element method, is to allow rapid calculation of residual stresses in order to perform real-time control of the process.

Analytical Residual Stress

A code has been developed to convert a temperature map produced by the FLASH method into a stress map that represents the thermal stresses induced by the last laser scan. The methodology given in [1] is valid for two-dimensional and semi-infinite medium. However,

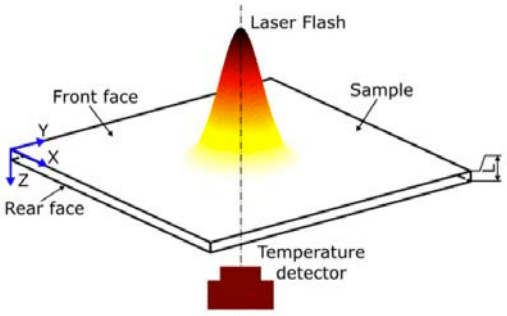

Figure 1: Principle of the FLASH method [2]

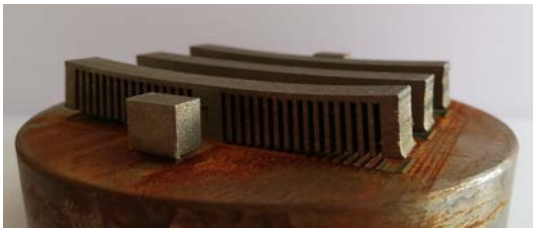

Figure 2: Observation of residual deformation, Printing temperature: 300°C

it is possible to extend this methodology to a 3D medium. Then the adaptation by [1] of the algorithm developed by [3] allows to compute residual stresses after relaxation of the thermal load.

Residual Stress Measurement

In order to validate the proposed model, tests have been realized on comb-like parts that are prone to bend under residual stresses after cutting (Figure 2). Several parts were printed at different ambiant temperatures (0, 200, 300°C) and for different lasing strategies. Then a strain map of the top of the parts was obtained via a structured light scanner.

Results

The printed comb-like parts highlighted the impact of printing temperature and scanning strategies (Figure 2).
This far, only the residual stress field of an elementary volume with a zig-zag lasing strategy is calculated by the code. This analytical approach allows in-depth interpretations of results with basis in the true mechanisms of the process. From this elementary volume, it would be possible to build a complex geometry with a checkerboard strategy in order to study the impact of the laser path on the residual stresses.

Further work

Work has still to be done to generalize this method to complex geometry and to be able to predict which scanning strategy will be the most efficient for each case. The challenge is to develop a scenario database that would allow the reduction of residual stresses in real time, thanks to an instrumentation of the printing machine.

REFERENCES

[1] O. Fergani, F. Berto, S.Y. Liang, Analytical modelling of residual stress in additive manufacturing In : *Procedia CIRP 45*, 171–174, 2016

[2] K. Ettaieb, S. Lavernhe, C. Tournier, Thermal simulation of scanning paths in LPBF additive manufacturing, II International Conference on Simulation for Additive Manufacturing, Pavia, Italie, 2019

[3] D.L. McDowell, An approximate algorithm for elastic/plastic 2D rolling/sliding contact In : *Wear*, 211:237-246, 1997

[4] Q. Chen, G. Guillemot, CA. Gandin, M. Bellet, Three-dimensional finite element thermomechanical modeling of additive manufacturing by selective laser melting for ceramic materials In : *Additive Manufacturing, 16*, 124-137, 2017

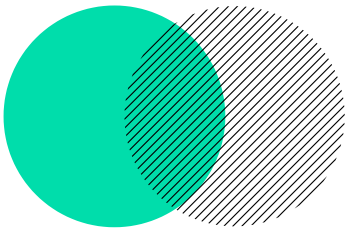

OPTIMISATION OF A VIRTUAL SINGLE-CAMERA STEREO-CORRELATION TEST OF DIGITAL IMAGES

ROLAND GODET - COLIN PRUVOT
MATTHIEU VITSE - STEPHANE ROUX - RENAUD GRAS

TER M1 2019-2020
FINAL DEFENCE OF RESEARCH PROJECTS
March 31, 2020, Cachan, France

école normale supérieure paris—saclay

TER M1 2019-2020
FINAL DEFENCE OF RESEARCH PROJECTS
March 31, 2020, Cachan, France

Optimisation of a virtual single-camera stereo-correlation test of digital images

R. Godet*, C. Pruvot*, M. Vitse*, S. Roux*, R. Gras◇

* Université Paris-Saclay, ENS Paris-Saclay, CNRS,
LMT - Laboratoire de Mécanique et Technologie, 94235, Cachan, France
e-mails : {roland.godet, colin.pruvot, matthieu.vitse, stephane.roux}@ens-paris-saclay.fr

◇ EikoSim
23 Avenue d'Italie, 75013 Paris
e-mail: renaud.gras@eikosim.com

KEYWORDS: Digital image multi-view correlation, virtual testing, stereo-correlation optimisation, calibration, robot arm

ABSTRACT

The term "Digital Image Correlation" (DIC) refers to the class of non-contacting methods that acquire images of an object, store them in digital form and perform image analysis to extract full-field shape, strain and/or motion measurements [1]. Significant advantages of a DIC technique for measuring strain and displacement lie in the fact that DIC is simple to use and cost effective compared to other techniques such as strain gauges or speckle interferometry. An essential part of this procedure is the camera calibration which characterises the transformation from pixel coordinates to 3D-world coordinates thanks to intrinsic and extrinsic parameters of the camera. As soon as the specimen shape is complex or when symmetry is broken (be it due to instabilities, geometry or to the strain mechanism itself), displacements have to be characterised in 3D [2]. A thoroughgoing characterisation requires that any surface of the specimen where displacements are to be measured should be observed. This implies operating with multiple points of view.

A virtual design approach was set up in a previous study [4] which offers the use of a single camera mounted on a robot arm (Figure 1). Using a single camera primarily aims at reducing the complexity of the set up. Then, modularity in the new setup can allow to run optimisation procedures on the stereo-correlation method. However, the robot is not able to come back exactly to the same position as it was before because of unpredictable mechanical clearances. Therefore, a procedure of re-calibration is needed after every movement of the arm. In order to study this "flying calibration", *Blender* [3] was mainly used partly because the virtual design was done in the software. It is a modular realistic 3D modelling software which is widely adopted in cinematography and more and more used for scientific applications.

This work focuses on this procedure where only extrinsic parameters has to be re-calculated because there are linked to the localisation of the camera in the world. On the contrary, intrinsic parameters depends on camera parameters which do not change if the camera moves. Moreover, another aim of this study is to validate a stereo-correlation mechanical testing virtually before doing it in real conditions. It could allow to check if the whole field of motion of the sample can be correctly measured in the simulated situation or not.

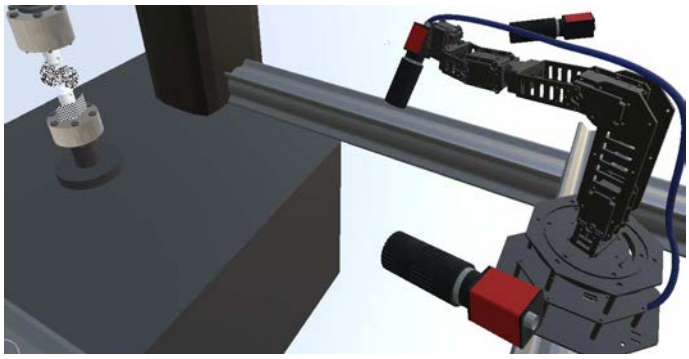

Figure 1: *Blender* environment - Single camera mounted on a robot arm with two possible positions pointing to the specimen

In order to study the impact of the re-positioning errors of the robot on the DIC procedure, a characterisation of it was done to be import into *Blender*. What is more, the software was utilised to create realistic images of a mechanical test with the camera viewpoint. At the end, an audit for compliance was performed between imposed motion field and the field calculated by EikoTwin, a partner software which assesses the strain of the sample by DIC.

Finally, this usage of *Blender* out of its initial functions permits to virtually validate a future stereo-correlation mechanical test. Furthermore, it should be possible to create a routine which optimises the camera positions in order to reduce measurement uncertainties.

REFERENCES

[1] M.A. Sutton, J.J. Orteu, H.W. Schreier *Image Correlation for Shape, Motion and Deformation Measurements - Basic Concepts,Theory and Applications*. Springer Edition, 2009.

[2] M. Vitse, *et al. Toward virtual design and optimization of a structural test monitored by a multi-view system*. The Journal of Strain Analysis for Engineering Design, 2020.

[3] Community, B. O. (2020). Blender - a 3D modelling and rendering package. Stichting Blender Foundation, Amsterdam. Retrieved from http://www.blender.org

[4] Q. Xu, *et al. Virtual/real dialogue to set up, control and optimize a single camera digital image stereo-correlation test*. Final defense of research projects, Cachan, 2019.